

Crystal growth and anisotropic resistivity of $\text{Bi}_2\text{Sr}_{2-x}\text{La}_x\text{CuO}_y$

N. L. Wang,* B. Buschinger, C. Geibel, and F. Steglich

Institut für Festkörperphysik, Technische Hochschule Darmstadt, Hochschulstraße 8, D-64289 Darmstadt, Germany

(Received 17 April 1996)

A number of $\text{Bi}_2\text{Sr}_{2-x}\text{La}_x\text{CuO}_y$ crystals with different doping levels in the phase diagram have been grown and characterized by x-ray-diffraction measurements. The anisotropic resistivity was measured using a generalization of the Montgomery method and was found to change in a systematic way. Our analysis indicates that for all the samples the in-plane transport is on the metallic side of the Ioffe-Regel criterion, but the out-of-plane transport is deeply on the insulating side of the Mott limit. The temperature dependence of c -axis resistivity $\rho_c(T)$ can be well understood from the incoherent hopping model proposed by Levin and co-workers. The evolution of $\rho_c(T)$ with reduction in doping level is related to the reducing of both the impurity- and boson-assisted hopping processes. [S0163-1829(96)04734-0]

I. INTRODUCTION

The understanding of high-temperature superconductivity requires careful study and understanding of the doping and temperature dependences of the normal-state properties of these materials. Among these properties, the anisotropic transport is of particular interest since it posed formidable challenge to theory.

To address the properties in the normal state, it is of advantage to investigate the cuprate superconductors with low critical temperatures. In this respect, the single-layer $\text{Bi}_2\text{Sr}_2\text{CuO}_y$ (Bi2201) materials provide the best candidate. Earlier studies^{1,2} have established that the in-plane resistivity is linear in T over the temperature range of 10–700 K, while the out-of-plane resistivity $\rho_c(T)$ is nonmetallic at low temperature. What is lacking so far is a systematic study of how the anisotropic resistivity evolves as a function of doping level. Our recent study revealed some correlation between the temperature variation of c -axis resistivity $\rho_c(T)$ and the in-plane resistivity $\rho_{ab}(T)$ in $\text{Bi}_2\text{Sr}_2\text{CuO}_y$ crystals with different Bi/Sr ratios and doped with Pb.³ However, it is not straightforward to compare the doping levels in these samples.

From the study of polycrystalline samples, it has been established that the entire phase diagram from the underdoped to the overdoped region can be achieved in the La-substituted Bi2201 system.^{4,5} Therefore, studies of the anisotropic transport properties in La-doped crystals are very promising to gain insight into the behavior with a change of doping level. Recently, we have grown a series of La-doped $\text{Bi}_2\text{Sr}_2\text{CuO}_y$ crystals. In this work we present the anisotropic resistivities measured by a generalization of the Montgomery method. Like the ceramic samples, the single crystals can cover the range from slightly underdoping to overdoping levels. The c -axis resistivity changes in a systematic way. A quantitative analysis suggests that the temperature dependence of c -axis resistivity $\rho_c(T)$ can be well understood from the incoherent hopping proposed by Levin and co-workers.^{6,7} The evolution of $\rho_c(T)$ with reduction in doping level is related to the reducing of both the impurity- and boson-assisted hopping processes.

II. CRYSTAL GROWTH AND CHARACTERIZATION

La-doped $\text{Bi}_2\text{Sr}_2\text{CuO}_y$ crystals were grown from a copper-oxide-rich melt in Al_2O_3 crucibles. We chose $\text{Bi}_2\text{Sr}_{2-x}\text{La}_x\text{Cu}_2\text{O}_y$ with $x=0, 0.025, 0.05, 0.1, 0.2$, and 0.3 as the nominal compositions in the melt. The mixture of the starting materials of Bi_2O_3 , SrCO_3 , La_2O_3 , and CuO was ground and fired at 790–820 °C for 12 h 2 or 3 times. The products were melted at 1000–1060 °C (depending on the La concentration) for 3 h, then cooled slowly to 850–880 °C at a rate of (1–2) °C/h, followed by a furnace cooling to room temperature. The crystal platelets were removed mechanically after breaking the crucibles. The sizes of the crystals become generally smaller with the increase of La concentration. But even for the $x=0.3$ compound, we can still obtain crystals with an area of 2 mm × 1 mm.

X-ray-diffraction (XRD) measurements were performed in order to check for the possible presence of secondary phases and to demonstrate the effect of La doping on the c -axis lattice parameter. It is found that all crystals, grown preferentially along the ab plane, were of the proper 2201 phase. There is no indication of a secondary phase. As examples, Fig. 1 shows the (0,0,1) XRD patterns for three samples with $x=0, 0.05$, and 0.2 . We find that the (0,0,1) peaks shift towards higher 2θ angles with the increase of La concentration, indicating the decrease of the c -axis lattice parameters. The inset of this figure illustrates the change of lattice parameter c as a function of nominal La concentration. The trend of c -axis parameter variation is consistent with the polycrystalline sample study.^{4,5} However, by comparing the c -axis lattice parameters with these results, we can conclude that the actual La contents of these crystals are larger than the nominal La concentrations. For example, the actual La content is around 0.3 for nominal $x=0.05$, while 0.5–0.6 for $x=0.3$. As demonstrated in Refs. 4 and 5, these La-substituted Bi2201 materials cover the entire region from underdoping to overdoping with the maximum T_c corresponding to $\text{La}=0.25\text{--}0.4$. We shall see below that our crystals, consistent with these reports, also pass at T_c maximum with the increase of La concentration. However, we refrained from determining directly the actual La content in our crystals.

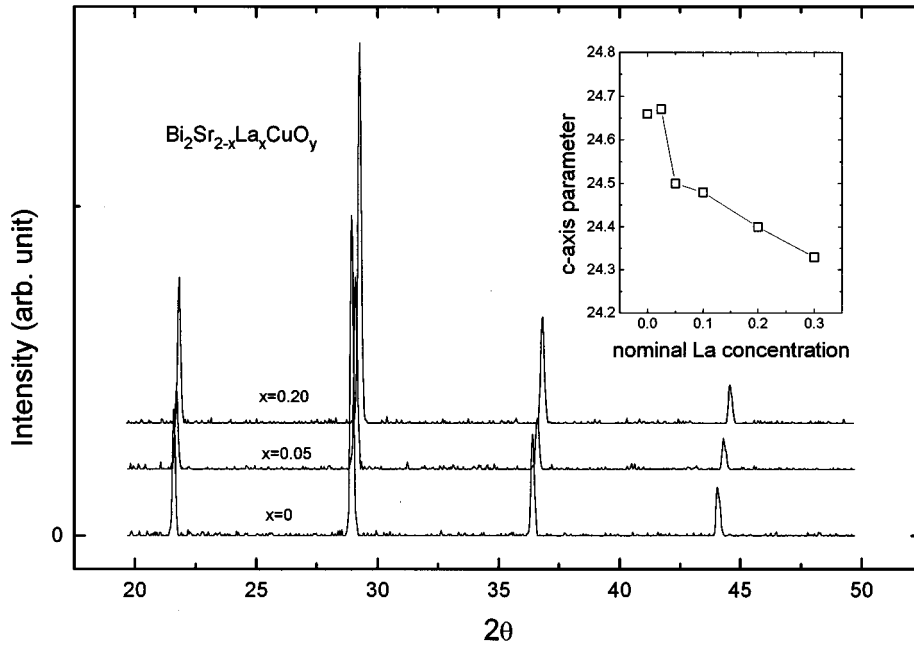


FIG. 1. X-ray-diffraction patterns for three Bi₂Sr_{2-x}La_xCuO_y crystals with $x=0$, 0.05, and 0.20 measured using 1.54 Å $K\alpha$ radiation. The inset shows the c -axis parameter as a function of nominal La concentration.

III. ANISOTROPIC RESISTIVITY

The anisotropic resistivity was measured using a generalization of the Montgomery method.⁸ The typical dimensions of crystals used to determine the resistivity were around 1 mm \times 0.6 mm \times 6 μ m with the shortest one along the c axis. The thickness of the crystal was determined by an Olympus BH2-UMA optical microscope. The silver-paint contacts were put on the ab plane. After firing the sample in air for 1 h at 500 °C, the contact resistance could be reduced to about 1–3 Ω . The contact configuration is shown in Fig. 2. Instead of the point contact in the original Montgomery method, we extended the contacts along the edges of samples to minimize the distortion effect of finite contact size along the c axis. The resistances, R_1 and R_2 , with the current nominally parallel and normal to the ab plane, respectively, were measured by an ac ($f=43$ Hz) method using a lock-in amplifier. The resistivity components, $\rho_{ab}(T)$ and $\rho_c(T)$, were then calculated from the ratio of R_2/R_1 in the thin sample limit of the Montgomery technique.

We shall first demonstrate that the temperature behavior of c -axis resistivity $\rho_c(T)$ can be very different from the measured resistance R_2 . As examples, Fig. 3 shows the measured resistances, R_1 and R_2 , for two samples with different nominal La concentrations. The main panel is a sample with $x=0.05$. It can be seen that R_2 is nonmetallic ($dR_2/dT < 0$) in the whole measured temperature range. However, after transforming to resistivity using the Montgomery technique, $\rho_c(T)$ exhibits a mixed behavior

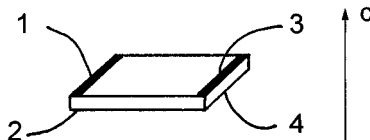


FIG. 2. The contact configuration for measuring anisotropic resistivity. $R_1 = V_{24}/I_{13}$, $R_2 = V_{34}/I_{12}$.

[$d\rho_c(T)/dT < 0$ at low T but $d\rho_c(T)/dT > 0$ at high T] (see Fig. 5). The inset of Fig. 3 is another sample with $x=0.30$. R_2 increases by two orders of magnitude as temperature drops from 290 to 10 K, while the transformed resistivity $\rho_c(T)$ only increases by a factor of 6 in the same temperature range (see Fig. 5). Therefore, the direct four-leads method for determining the c -axis resistivity is not accurate enough. An analysis for the reasons of different temperature behaviors between R_2 and $\rho_c(T)$ can be found in Ref. 9.

The anisotropic resistivities data measured by this method on more samples are shown in Figs. 4 and 5. Before comparing the temperature behaviors, we pay attention to the change of superconducting transition temperatures in these

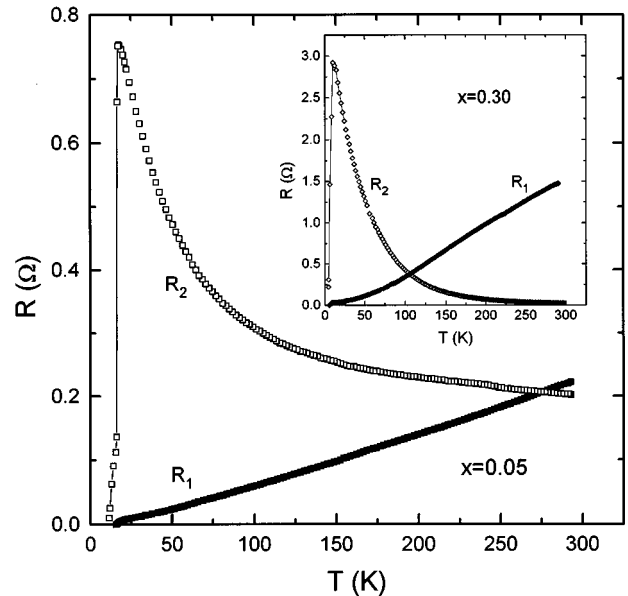


FIG. 3. The measured resistances R_1 and R_2 for two La-doped samples. The main panel is a sample with nominal $x=0.05$. The inset is a sample with $x=0.30$.

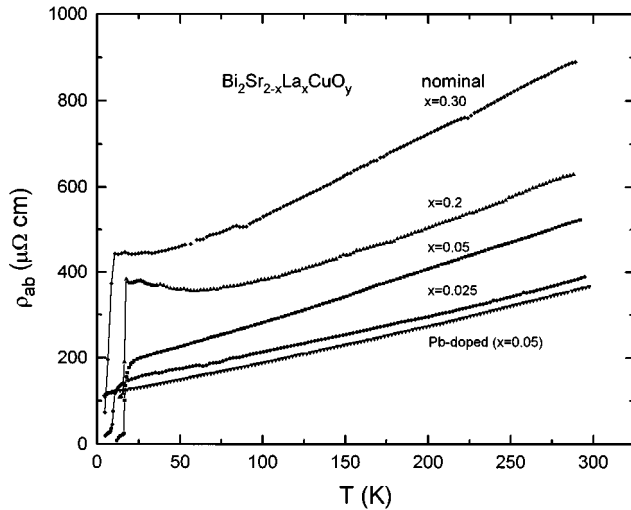


FIG. 4. The in-plane resistivity $\rho_{ab}(T)$ of the La-doped Bi2201 crystals and a lead-doped one.

La-doped crystals. Our undoped Bi2201 crystals generally show superconducting transitions at temperatures between 4 and 7 K (not shown in this figure). T_c increases with the addition of La. T_c is 11 K at the nominal La concentration $x=0.025$, and reaches 18 K when $x=0.05$. However, as x changes from 0.05 to 0.2, we did not observe much change in T_c . This is consistent with the report in polycrystalline samples in which T_c keeps nearly constant when $0.25 < x < 0.5$. T_c changes back to 10 K when $x=0.3$, suggesting that this sample has already passed the maximum

T_c . The variation of superconducting transition temperatures with the increase of La concentration indicates that these crystals have covered the range from overdoping to slightly underdoping in the phase diagram as a result of hole filling due to the substitution of La^{3+} for Sr^{2+} . This argument is supported by the variation of temperature dependences of the anisotropic resistivities. It should be mentioned that the hole filling effect does not take place in a simple way. As the substitution of La^{3+} for Sr^{2+} normally results in incorporation of additional O ions,⁴ this will partly compensate the charge difference. We add a lead-doped sample with nominal composition of $\text{Bi}_{2-x}\text{Pb}_x\text{Sr}_2\text{Cu}_2\text{O}_y$ ($x=0.05$) to this series. The description of the growth of this crystal can be found in Ref. 3. A previous study¹⁰ has shown that doped lead has the valence state 2+ rather than 4+ in these 2201 materials. Thus the substitution of Pb^{2+} for Bi^{3+} will result in the increase of carrier concentration. Our measurements indeed show that the Pb-doped sample has the least resistivity and anisotropic ratio.

The in-plane resistivities $\rho_{ab}(T)$ are shown in Fig. 4. The La concentration $x=0.05$ sample shows the highest T_c (~ 18 K) with a linear- T dependence in the normal state. This indicates that the sample is nearly optimally doped. The $x=0.025$ sample and the Pb-doped samples have lower T_c values and magnitudes of resistivity, and exhibit a superlinear T -dependence. This superlinear T -dependent $\rho_{ab}(T)$ is a feature of overdoped samples and has been observed in various cuprate systems, for example, in Tl2201 (Ref. 11) and La214 (Ref. 12) materials. In contrast, the samples with higher La concentrations, like $x=0.2$ and $x=0.3$, have

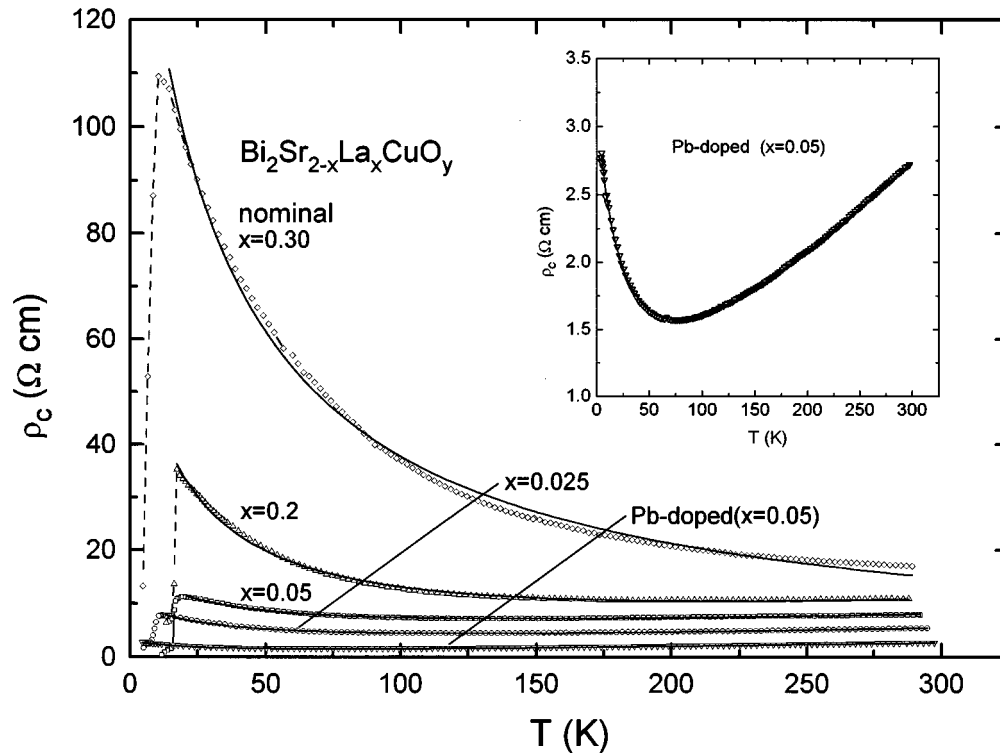


FIG. 5. The out-of-plane resistivity $\rho_c(T)$ for the same crystals as in Fig. 4. The solid curves are fits of $\rho_c(T)$ data to $\rho_c = a_0 + aT + 1/(c + bT)$. The ρ_c vs T curve for the same lead-doped crystal is replotted in the inset to show more clearly the temperature behavior.

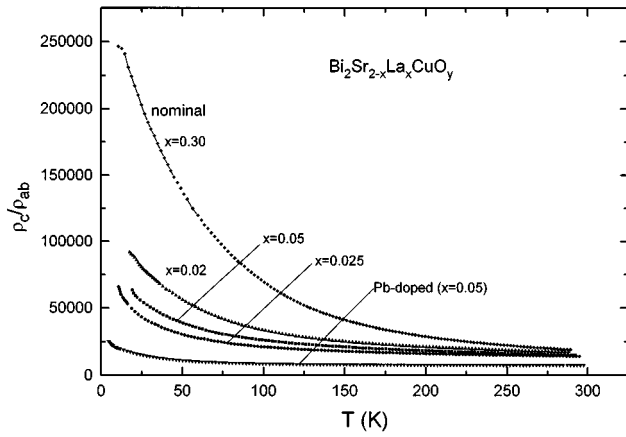


FIG. 6. The anisotropy ratios ρ_c/ρ_{ab} vs T for the same crystals as in Fig. 4.

higher resistivity. At low T , $\rho_{ab}(T)$ becomes flat or even shows an upturn. This is in accord with the above conclusion that they are already in the slightly underdoped region. The more obvious upturn in $\rho_{ab}(T)$ at low T for the $x=0.2$ sample may imply that the disorder in this sample is stronger than in the $x=0.3$ sample.

The out-of-plane resistivities of the above samples are shown in Fig. 5. A prominent feature is that $\rho_c(T)$ shows a mixed temperature dependence, i.e., $\rho_c(T)$ has a positive slope ($d\rho_c/dT > 0$) at high T but a negative slope ($d\rho_c/dT < 0$) at low T . In between, $\rho_c(T)$ has a minimum. This feature is shown rather clearly for a Pb-doped sample by replotting the ρ_c vs T curve in the inset of this figure. A systematic evolution of $\rho_c(T)$ with the reduction of doping level in these samples is observed. That is, the magnitude of the resistivity increases rapidly, and the temperature T_{\min} corresponding to the minimum ρ_c shifts towards higher temperature. T_{\min} is about 75 K for the Pb-doped sample, 100 K for the La $x=0.025$ sample, 120 K for $x=0.05$, 175 K for $x=0.2$, respectively. For the $x=0.3$ sample, $T_{\min} > 300$ K.

Figure 6 shows the temperature dependence of the anisotropy ratio ρ_c/ρ_{ab} for those samples. The following features are worth mentioning. First, the anisotropy ratio is rather large. All samples exceed 10^4 . Second, ρ_c/ρ_{ab} depends on T for all the samples. This implies that the mechanisms governing the transports along and perpendicular to the CuO plane are different. Third, the anisotropy ratio increases further as the doping level decreases. For the La $x=0.30$ sample, the anisotropy ratio has nearly reached 2.5×10^5 at low T .

The remarkable difference between the temperature dependence of ρ_{ab} and ρ_c is still one of the least understood properties. We shall first demonstrate that the conventional Bloch-Boltzmann theory cannot explain such difference. Within the framework of Boltzmann transport, the expression for anisotropic resistivities can be derived by solving the linear Boltzmann equation in the relaxation-time (τ) approximation

$$e\mathbf{E} \cdot \mathbf{v}(\mathbf{k}) \partial f_0 / \partial \varepsilon = (f - f_0) / \tau, \quad (1)$$

and by calculating the electric current density

$$\mathbf{J} = 2e \int \mathbf{v}(\mathbf{k}) (f - f_0) d^3k / (2\pi)^3. \quad (2)$$

Here f_0 is the equilibrium Fermi distribution function, $(f - f_0)$ the deviation from the distribution function due to the electric field \mathbf{E} and the scattering which transfers carriers from one band state to the others, and $\mathbf{v}(\mathbf{k}) = \hbar^{-1} \partial \varepsilon(\mathbf{k}) / \partial \mathbf{k}$ is the group velocity. To address the conductivity along the c axis, the energy dispersion relationship must include the dispersion along the c axis. The simplest case is to assume the dispersion of $\varepsilon(\mathbf{k}) = (\hbar \mathbf{k}_{ab})^2 / (2m_{ab}^*) + (\hbar k_c)^2 / (2m_c^*)$, then it is easy to obtain the following Drude anisotropic resistivities:

$$\rho_{ab} = m_{ab}^* / n e^2 \tau \quad (3)$$

and

$$\rho_c = m_c^* / n e^2 \tau, \quad (4)$$

where n is the density of charge carriers. Since both ρ_{ab} and ρ_c are inversely proportional to τ , they must have the same T dependence. Of course, the expression for ρ_{ab} and ρ_c can be different if a different band energy dispersion relationship is assumed. However, it does not appear possible to obtain simultaneously a nonmetallic conduction along the c axis and a metallic one within the plane within this theory. For this reason, it does not seem to be reasonable to ascribe the large anisotropic ratio ρ_c/ρ_{ab} to the anisotropic effective masses along different directions.

In fact, the very large anisotropic ratio suggests that the energy dispersion along the c axis is negligible. Suppose that the Fermi surface is cylindrically shaped, we can use the above Drude in-plane equation to roughly estimate the in-plane transport parameters ($k_F l$). For this purpose, we change Eq. (3) into another form. For a quasi-two-dimensional electron system with cylinder-shaped Fermi surface, the carrier density $n = (k_F^2 / 2\pi) / d_c$, where k_F is the Fermi wave vector, $d_c = c/2$ is the periodic length in the c axis. Noticing $1/\tau = v/l$, $m_{ab}^* v = \hbar k_F$, then Eq. (3) can be written as

$$\rho_{ab} = (\hbar / e^2) (c/2) / k_F l. \quad (5)$$

From this equation, the in-plane transport parameter $k_F l$ at 25 K is estimated to be 26 for the Pb-doped sample, 17 for the $x=0.05$ La-doped sample, and 7 for the $x=0.30$ La-doped sample (which has the highest magnitude of resistivity in this series), respectively. The large metallic parameters $k_F l$ place these samples into the metallic side of the Ioffe-Regel criterion ($k_F l > 1$) for the in-plane transport. In contrast to this, we find that the out-of-plane conductivity is far beyond the Mott minimum conductivity. In terms of the theories developed by Mott, the minimum conductivity is given by¹³

$$\sigma_{\min} = 0.03 e^2 / (\hbar d_c), \quad (6)$$

the value of the constant could be somewhat different depending on the Anderson localization criterion. Inserting the d_c value into this equation, we get $\sigma_{\min} \sim 58 (\Omega \text{ cm})^{-1}$. Therefore, the ρ_c data for all the samples are deeply on the insulating side of the Mott limit. The above analysis indi-

catates definitely that the conduction along the c axis is not a coherent band transport, though it is possible within the ab plane.

There have been several theoretical models aiming to elucidate the temperature dependence of c -axis resistivity $\rho_c(T)$. For example, Kumar and Jayannavar¹⁴ proposed a model in which they took the in-plane electron dynamics as bandlike, characterized by a Boltzmann mean free lifetime τ , i.e., the in-plane resistivity had the usual Drude relation (3), but the c -axis transport as an interplanar tunneling between neighboring layers which were blocked by intraplanar inelastic scattering. This model gives the same temperature dependence for the c -axis resistivity as that for the in-plane resistivity, and is, therefore, in contrast to our experimental results. The famous “confinement” theory proposed by Anderson,¹⁵ asserting that each CuO_2 layer is a spin-charge-separated Luttinger liquid, gives a semiconducting T dependence of c -axis resistivity with $\rho_c(T) \sim 1/T$. This theory can qualitatively explain the nonmetallic $\rho_c(T)$ behavior, but unfortunately, cannot be quantitatively fit well to our data. In the following, we shall illustrate that our $\rho_c(T)$ data can be well explained from the incoherent transport model proposed by Levin and co-workers.^{6,7} According to this model, the c -axis conductivity is contributed from three hopping processes: direct interlayer quasiparticle hopping which is due to the wave function overlap, hopping assisted through static disorder (impurity), and hopping assisted through inelastic boson-mediated (e.g., phonon-mediated) scattering. The conductivity expressions for these processes are summarized as follows:

$$\sigma_c^{\text{direct}} = \sigma_0 N_0 t_{\perp}^2 (\tau_{ab} / \pi \hbar) = 1/(b'T + c'), \quad (7)$$

$$\sigma_c^{\text{imp}} = \sigma_0 N_0^2 \ll |V_{k-k'}|^2 \gg_k \gg_{k'} = c, \quad (8)$$

$$\sigma_c^{\text{inel}} = \sigma_0 N_0^2 \ll |g_{k-k'}|^2 \gg_k \gg_{k'} I(T) = bI(T), \quad (9)$$

and

$$\sigma_c = \sigma_c^{\text{direct}} + \sigma_c^{\text{imp}} + \sigma_c^{\text{inel}} = bI(T) + c + 1/(b'T + c'). \quad (10)$$

Here, b , c , b' , and c' are constant, $I(T)$ is the spectrum function of the boson assisting the interlayer hopping. To capture the features of the spectrum function, Rojo and Levin⁶ took the Bloch-Grüneisen form for $I(T)$. At high T ($> \Theta/5$, Θ is the Debye temperature), $I(T) \propto T$. While Radtke and Levin⁷ used the Einstein spectrum for $I(T)$, i.e., $I(T) \propto (T_0/T)/\sinh^2(T_0/T)$. In fact, if $T_0/T \ll 1$, this Einstein spectrum is also reduced to $I(T) \propto T$. As the in-plane resistivity could be proportional to T down to the superconducting transition temperature, we shall simply use $I(T) \propto T$ in our fitting. For the extremely anisotropic materials, like Bi cuprates, the direct interlayer hopping can be ignored.¹⁶ It is

TABLE I. The fit parameters a_0 , a , b , and c for different samples in Fig. 5.

Samples	a	a_0	c	b
Pb-doped (0.05)	0.008	0.15	0.34	1.14×10^{-2}
La-doped $x=0.025$	0.012	1.27	0.10	3.72×10^{-3}
$x=0.05$	0.013	2.94	0.07	2.43×10^{-3}
$x=0.20$	0.023	0.1	0.014	7.90×10^{-4}
$x=0.30$	0	0	0.0069	2.05×10^{-4}

possible for any measurement to pick up an in-plane component of the resistivity tensor. This could be caused by the short circuits due to the crystal imperfections or external misalignment of contacts. In fact, the randomly distributed defects of single crystals have been observed in many published papers.¹⁷ So we add a linear term ($a_0 + aT$) to the c -axis resistivity. We use the following equation to fit our resistivity data:

$$\rho_c = a_0 + aT + 1/(c + bT). \quad (11)$$

The last term in the equation is the intrinsic resistivity along the c axis and corresponds to the impurity- and boson-assisted hopping processes. As shown in Fig. 5, this equation fits the data fairly well in a wide range of temperature. The fitting parameters are listed in Table I. There is little change in the parameter a in this series of samples. However, both the parameters c and b decrease systematically with the reduction of doping level. This implies that the evolution of the c -axis resistivity is caused by the further reducing of both the impurity- and boson-assisted hopping processes. Therefore, our experimental data can be well understood within this incoherent model.

In summary, we have grown successfully La-doped Bi2201 crystals with different doping levels in the phase diagram. The anisotropic resistivity was measured using a generalization of the Montgomery method and found to change in a systematic way. Our analysis indicates that for all the samples, the in-plane transport is on the metallic side of the Ioffe-Regel criterion, but the out-of-plane transport is deeply on the insulating side of the Mott limit. The temperature dependence of c -axis resistivity $\rho_c(T)$ can be well understood from the incoherent hopping model proposed by Levin and co-workers. The evolution of $\rho_c(T)$ with reduction in doping level is caused by the reducing of both the impurity- and boson-assisted hopping processes.

ACKNOWLEDGMENTS

We have benefited from discussions with Dr. Y. Ando and Dr. R. J. Radtke. The financial support from Alexander von Humboldt Foundation is greatly acknowledged.

*Permanent address: Department of Physics, University of Science and Technology of China, Hefei 230026, People's Republic of China.

¹S. Martin, A. T. Fiory, R. M. Fleming, L. F. Schneemeyer, and J. V. Waszczak, Phys. Rev. B **41**, 846 (1990).

²X. H. Hou, W. J. Zhu, J. Q. Li, J. W. Li, J. W. Xiong, F. Wu, Y.

Z. Hang, and Z. X. Zhao, Phys. Rev. B **50**, 496 (1994).

³N. L. Wang, C. Geibel, and F. Steglich, Physica C **260**, 305 (1996).

⁴W. Bauhofer, H. Mattausch, R. K. Kremer, P. Murugaraj, and A. Simon, Phys. Rev. B **39**, 7244 (1989).

⁵N. R. Khasanova and E. V. Antipov, Physica C **246**, 241 (1995).

- ⁶A. G. Rojo and K. Levin, Phys. Rev. B **48**, 16 861 (1993).
- ⁷R. J. Radtke and K. Levin, Physica C **250**, 282 (1995).
- ⁸H. C. Montgomery, J. Appl. Phys. **42**, 2971 (1971), and accompanying paper by B. F. Logan, S. O. Rice, and R. F. Wick, *ibid.* **42**, 2975 (1971).
- ⁹S. J. Hagen, T. W. Jing, Z. Z. Wang, J. Horvath, and N. P. Ong, Phys. Rev. B **37**, 7928 (1988).
- ¹⁰C. C. Torardi, E. M. McCarron, P. L. Gai, J. P. Parise, J. Ghoroghchian, D. B. Kang, M.-H. Whangbo, and J. C. Barry, Physica C **176**, 347 (1991).
- ¹¹Y. Kubo, Y. Shimakawa, T. Manako, and H. Igarashi, Phys. Rev. B **43**, 7875 (1991).
- ¹²H. Takagi, B. Batlogg, H. L. Kao, J. Kwo, R. J. Cava, J. J. Krajewski, and W. F. Peck, Jr., Phys. Rev. Lett. **69**, 2975 (1992).
- ¹³See, for example, N. F. Mott, in *The Metallic and Nonmetallic States of Matter*, edited by P. P. Edwards and C. N. R. Rao (Taylor & Francis, London, 1985), p. 1.
- ¹⁴N. Kumar and A. M. Jayannavar, Phys. Rev. B **45**, 5001 (1992).
- ¹⁵P. W. Anderson and Z. Zou, Phys. Rev. Lett. **60**, 132 (1988); P. W. Anderson, Science **256**, 1526 (1992).
- ¹⁶R. J. Radtke, V. N. Kostur, and K. Levin, Phys. Rev. B **53**, 522 (1996).
- ¹⁷See, for example, R. Jin, H. R. Ott, and D. P. Grindatto, Physica C **250**, 395 (1995).